Spring 5-1-2020

Changes in the Scattering Phase Shifts for Partial Waves of Ultracold Particles at Different Energies

Kaaviyan Faezi
kf@uconn.edu

Changes in the Scattering Phase Shifts for Partial Waves of Ultracold Particles at Different Energies

Kaaviyan Faezi

Department of Physics, University of Connecticut

Thesis Advisor: Dr. Robin Côté

Spring 2020

At low energies, scattering phase shifts, the difference in phases between the incoming and outgoing spherical waves in scattering, for different partial waves follow a similar pattern. The phase shift curves, which are a function of the angular momentum quantum number ℓ for different scattering energy, obtain resonances after reaching their maxima, and as energy is increased, these resonances become smaller and eventually disappear. Using numerical methods involving the use of Chebyshev polynomials, we solve the wave equation for a scattering potential to obtain the radial equation. From the radial equation we then find the scattering phase shift for a particular energy and partial wave. The numerical methods for this project are used through code in MATLAB. By analyzing the phase shifts across different partial waves, we seek to find a relation between the scattering energy and the shape of the phase shift curves related to the disappearance of resonances.

I. Introduction

Scattering theory is based off of the concepts of classical scattering. In classical scattering theory, a particle incident on a scattering center has an incoming energy E and impact parameter b (the distance between the initial trajectory of the incoming particle and the scattering center), and it has an outgoing scattering angle θ. Using classical scattering, θ can be calculated given E and b. In classical elastic scattering, the cross section σ represents the area of the scattering center that will cause scattering in a collision with the incoming particle. In non-elastic cases and quantum scattering theory, the scattering cross section is a measure of probability that scattering will occur in a collision between the incoming particle and the scattering center. The cross section in classical scattering theory can be calculated by considering that particles incident within an infinitesimal patch of cross-sectional area $d\sigma$ will scatter into an infinitesimal solid angle $d\Omega$. The proportionality factor $\frac{d\sigma}{d\Omega}$ is called the differential scattering cross section. The total cross section is found by taking the integral of the differential scattering cross section over all solid angles:

$$\sigma = \int \frac{d\sigma}{d\Omega} d\Omega \tag{1}$$

In quantum scattering theory, an incident plane wave is considered instead of an incident particle. The plane wave is typically represented by $\psi(z) = Ae^{ikz}$ traveling in the z direction. This wave interacts with a scattering potential, producing an outgoing spherical wave. The spherical wave is calculated by finding solutions to the Schrödinger equation of the general form

$$\psi(r, \theta) \approx A\left(e^{ikz} + f(\theta)\frac{e^{ikr}}{r}\right) \tag{2}$$

where r is large and f is the amplitude of the outgoing spherical wave. The wave number k is related to the energy of the incident particle E by

$$k = \frac{\sqrt{2mE}}{\hbar} \tag{3}$$

where $\hbar$ is the reduced Planck constant and m is the mass of the particle. Solving for the scattering amplitude $f(\theta)$ will give the probability of scattering in a given direction θ. This value is related to the differential cross section by the equation

$$\frac{d\sigma}{d\Omega} = |f(\theta)|^2 \tag{4}$$

The scattering amplitude can be calculated using partial wave analysis. The Schrödinger equation for a spherically symmetrical potential $V(r)$ produces the solutions

$$\psi(r,\theta,\phi) = R(r)Y_\ell^m(\theta,\phi) \tag{5}$$

where Y_ℓ^m is a spherical harmonic and $u(r) = rR(r)$ satisfies the radial equation:

$$-\frac{\hbar^2}{2m}\frac{d^2u}{dr^2} + \left(V(r) + \frac{\hbar^2}{2m} + \frac{\ell(\ell+1)}{r^2}\right)u = Eu \tag{6}$$

At large r ($kr \gg 1$), the potential and centrifugal contribution become negligible, so $\frac{d^2u}{dr^2} \approx -k^2u$. The general solution is $u(r) = Ce^{ikr} + De^{-ikr}$. However, since the first term represents an outgoing spherical wave, and the second term represents an incoming spherical wave, $D = 0$ for the scattered wave. Thus $R(r) \sim \frac{e^{ikr}}{r}$. If r is slightly smaller than the previous case such that the potential is negligible, but the centrifugal term is not, then the radial equation becomes

$$\frac{d^2u}{dr^2} - \frac{\ell(\ell+1)}{r^2}u = -k^2u \tag{7}$$

and the general solution becomes a combination of spherical Bessel functions

$$u(r) = Arj_\ell(kr) + Brn_\ell(kr) \tag{8}$$

In order to find linear combinations analogous to the incoming and outgoing spherical wave terms, spherical Hankel functions are used instead of spherical Bessel functions:

$$h_\ell^{(1)}(x) = j_\ell(x) + in_\ell(x); h_\ell^{(2)}(x) = j_\ell(x) - in_\ell(x) \tag{9}$$

This makes the exact wave function outside the scattering region

$$\psi(r,\theta,\phi) = A\left(e^{ikz} + \sum_{\ell,m} C_{\ell,m}h_\ell^{(1)}(kr)Y_\ell^m(\theta,\phi)\right) \tag{10}$$

where the first term represents the incident plane wave, and the second summation term represents the scattered wave. In the case of a spherically symmetric potential, all terms with $m \neq 0$ go to zero.

$$Y_{\ell}^{0}(\theta,\phi) = \sqrt{\frac{2\ell+1}{4\pi}}P_{\ell}(\cos\theta) \tag{11}$$

where P_ℓ is the ℓth Legendre polynomial. Defining the expansion coefficient in the $m = 0$ case as $C_{\ell,0} = i^{\ell+1}k\sqrt{4\pi(2\ell+1)}a_\ell$, the wave function becomes

$$\psi(r,\theta) = A\left(e^{ikz} + k\sum_{\ell=0}^{\infty} i^{\ell+1}(2\ell+1)a_\ell h_\ell^{(1)}(kr)P_\ell(\cos\theta)\right) \tag{12}$$

a_ℓ is called the ℓth partial wave amplitude. For large r, the behavior of the Hankel function causes the wave function to approach

$$\psi(r,\theta) \approx A\left(e^{ikz} + f(\theta)\frac{e^{ikr}}{r}\right) \tag{13}$$

where

$$f(\theta) = \sum_{\ell=0}^{\infty}(2\ell+1)a_\ell P_\ell(\cos\theta) \tag{14}$$

Hence this makes the total cross section

$$\sigma = 4\pi\sum_{\ell=0}^{\infty}(2\ell+1)|a_\ell|^2 \tag{15}$$

In order to solve for the partial wave amplitudes, the wave function must be written completely in spherical coordinates. The explicit expansion of a plane wave in terms of spherical waves is Rayleigh's formula:

$$e^{ikz} = \sum_{\ell=0}^{\infty} i^{\ell}(2\ell+1) j_{\ell}(kr) P_{\ell}(\cos\theta) \tag{16}$$

This formula can be used to express the wave function solely in spherical coordinates:

$$\psi(r,\theta) = A \sum_{\ell=0}^{\infty} i^{\ell}(2\ell+1)\left(j_{\ell}(kr) + ika_{\ell}h_{\ell}^{(1)}(kr)\right) P_{\ell}(\cos\theta) \tag{17}$$

In this case, the incident plane wave has no angular momentum in the z direction, but it contains all values of the total angular momentum for every partial wave. Each partial wave scatters independently with no change in amplitude since angular momentum is conserved by a spherically symmetric potential. However, the partial waves scatter with change in phase. In the case of no potential, the ℓth partial wave is

$$\psi_0^{\ell} = Ai^{\ell}(2\ell+1) j_{\ell}(kr) P_{\ell}(\cos\theta) \tag{18}$$

For large r ($kr \gg 1$), this becomes

$$\psi_0^{\ell} \approx A\frac{(2\ell+1)}{2ikr}\left(e^{ikr} - (-1)^{\ell}e^{-ikr}\right) P_{\ell}(\cos\theta) \tag{19}$$

e^{ikr} represents the outgoing wave, and $(-1)^{\ell}e^{-ikr}$ represents the incoming wave. When a scattering potential is introduced, the incoming wave is unchanged, but the outgoing wave receives a phase shift δ_{ℓ}:

$$\psi^{\ell} \approx A\frac{(2\ell+1)}{2ikr}\left(e^{i(kr+2\delta_{\ell})} - (-1)^{\ell}e^{-ikr}\right) P_{\ell}(\cos\theta) \tag{20}$$

By comparing the asymptotic version of (12):

$$\psi^{\ell} \approx A\left(\frac{(2\ell+1)}{2ikr}\left(e^{ikr} - (-1)^{\ell}e^{-ikr}\right) + \frac{(2\ell+1)}{r}a_{\ell}e^{ikr}\right) P_{\ell}(\cos\theta) \tag{21}$$

with (20), the partial wave amplitudes can be found in terms of the phase shifts:

$$a_{\ell} = \frac{1}{2ik}\left(e^{2i\delta_{\ell}} - 1\right) = \frac{1}{k}e^{i\delta_{\ell}}\sin(\delta_{\ell}) \tag{22}$$

It follows from (14) that

$$f(\theta) = \frac{1}{k}\sum_{\ell=0}^{\infty}(2\ell+1)e^{i\delta_\ell}\sin(\delta_\ell)\,P_\ell(\cos\theta) \tag{23}$$

and (15) that

$$\sigma = \frac{4\pi}{k^2}\sum_{\ell=0}^{\infty}(2\ell+1)\sin^2(\delta_\ell) \tag{24}$$

II. Numerical Approach

The wave equation can be solved numerically for the radial equation using a method which involves the use of Chebyshev polynomials. The Chebyshev polynomial of degree n, $T_n(x)$, has n zeroes in the interval $[-1,1]$ at the points

$$x_k = \cos\left(\frac{\pi\left(k-\frac{1}{2}\right)}{n}\right), k = 1,2,\dots,n \tag{25}$$

and has $n+1$ extrema at the points

$$\tilde{x}_k = \cos\left(\frac{\pi k}{n}\right), k = 0,1,\dots,n \tag{26}$$

The Chebyshev polynomials are orthogonal in the interval $[-1,1]$ and satisfy discrete orthogonality relationships. Thus if x_k are the N zeroes of $T_N(x)$ according to (25), then

$$\sum_{k=1}^{N} T_i(x_k)T_j(x_k) = \alpha_i\delta_{ij} \tag{27}$$

where $i,j < N$ and $\alpha_i = \begin{cases}\frac{N}{2}, i \neq 0\\ N, i = 0\end{cases}$. Similarly if $\tilde{x}_k$ are the $N+1$ extrema according to (26), then the discrete orthogonality relation is

$$\sum_{k=0}^{N''} T_i(\tilde{x}_k)T_j(\tilde{x}_k) = \beta_i\delta_{ij} \tag{28}$$

where $i, j < N$ and $\beta_i = \begin{cases} \frac{N}{2}; i \neq 0, N \\ N; i = 0, N \end{cases}$. The summation with double primes denotes a sum with both the first and last terms halved. A continuous and bounded function $f(x)$ can be approximated in $[-1,1]$ by either

$$f(x) \approx \sum_{j=0}^{N-1\prime} a_j T_j(x) \tag{29}$$

or

$$f(x) \approx \sum_{j=0}^{N\prime\prime} b_j T_j(x) \tag{30}$$

where

$$a_j = \frac{2}{N} \sum_{k=1}^{N} f(x_k) T_j(x_k)\,; j = 0, \ldots, N-1 \tag{31}$$

and

$$b_j = \frac{2}{N} \sum_{k=0}^{N\prime\prime} f(\tilde{x}_k) T_j(\tilde{x}_k)\,; j = 0, \ldots, N \tag{32}$$

The summation with a single prime denotes a sum with the first term halved. (29) is exact at $x = x_k$ according to (25), and (30) is exact at $x = \tilde{x}_k$ according to (26). By expanding (25) and (26), $f'(x)$ can be approximated as

$$f'(x) \approx \sum_{k=1}^{N} f(x_k) \frac{2}{N} \sum_{j=0}^{N-1\prime} T_j(x_k) T_j'(x) \tag{33}$$

or

$$f'(x) \approx \sum_{k=0}^{N\prime\prime} f(\tilde{x}_k) \frac{2}{N} \sum_{j=0}^{N\prime\prime} T_j(\tilde{x}_k) T_j'(x) \tag{34}$$

In addition, $\int_{-1}^{x} f(t)\,dt$ can be approximated as

$$\int_{-1}^{x} f(t)\,dt \approx \sum_{k=1}^{N} f(x_k)\frac{2}{N}\sum_{j=0}^{N-1\prime} T_j(x_k)\int_{-1}^{x} T_j(t)\,dt \tag{35}$$

or

$$\int_{-1}^{x} f(t)\,dt \approx \sum_{k=0}^{N\prime\prime} f(\tilde{x}_k)\frac{2}{N}\sum_{j=0}^{N\prime\prime} T_j(\tilde{x}_k)\int_{-1}^{x} T_j(t)\,dt \tag{36}$$

This method can be used to solve linear integral equations, integro-differential equations, and ordinary differential equations. By increasing N, more exact values can be found for the solutions of the differential equation, and the numerical approximation will be closer to the exact result. This Chebyshev method can be used to solve the wave equation in the case of a scattering potential in order to find the radial equation. In the case of scattering in a spherically symmetric potential the ℓth radial wavefunction takes the form

$$R_\ell(r) = e^{i\delta_\ell}\big(\cos\delta_\ell\, j_\ell(kr) - \sin\delta_\ell\, y_\ell(kr)\big) \tag{37}$$

The logarithmic derivative of the ℓth radial wavefunction is given by

$$\beta_\ell = kr\left(\frac{\cos\delta_\ell\, j_\ell'(kr) - \sin\delta_\ell\, y_\ell'(kr)}{\cos\delta_\ell\, j_\ell(kr) - \sin\delta_\ell\, y_\ell(kr)}\right) \tag{38}$$

and thus the phase shift can be found by the equation

$$\tan\delta_\ell = \frac{krj_\ell'(kr) - \beta_\ell j_\ell(kr)}{kry_\ell'(kr) - \beta_\ell y_\ell(kr)} \tag{39}$$

Therefore, by obtaining the radial equation using the numerical Chebyshev method, the phase shift can be found as well. This is computed using code in MATLAB. However, since $\tan\delta_\ell$ is calculated in order to find δ_ℓ, the value of δ_ℓ found is always in the interval $(-\pi,\pi]$ and correct modulo π. In order to develop continuous plots of the phase shift values, the code manually corrects for continuity by adding or subtracting π if it detects a difference of greater than $\frac{\pi}{2}$ between two consecutive values. However, some resonances in the phase shifts can be missed if the difference between two consecutive values is large enough to seem small modulo π. These resonances can be found and shown on the plots if the step size between two phase shift values is decreased.

III. Physical System

The specific case examined using the Chebyshev numerical method is the case of an atom of Cesium (Cs) as the incoming particle with an atomic mass of 132.90545 u. The scattering potential used is an inter-atomic potential with long-range behavior of the type $V(R) \sim -\frac{C_6}{R^6}$. It took the form of

$$V(R) = C_{wall} e^{-\frac{R}{R_{wall}}} - \frac{C_6}{R^6 + R_{core}^6} - C_x e^{-\frac{R}{R_x}} \tag{40}$$

with $C_{wall} = 60, R_{wall} = 1, R_{core} = 7, C_6 = 6877, C_x = 0.08, R_x = 5$. The potential is shown in FIG. 1, and the interval is reduced in FIG. 2 to better show the asymptotic behavior of the potential.

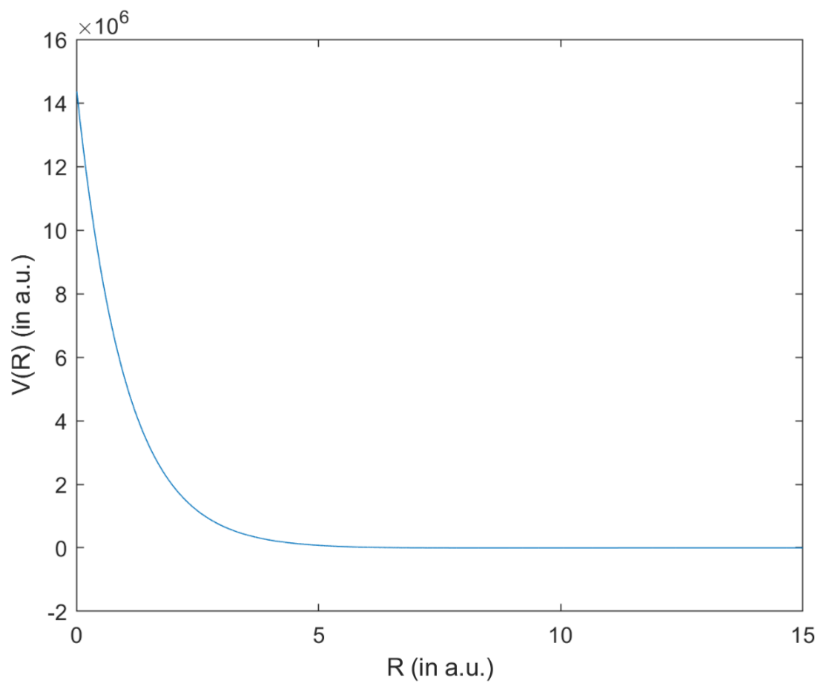

FIG. 1. Potential in (40) as a function of *R*

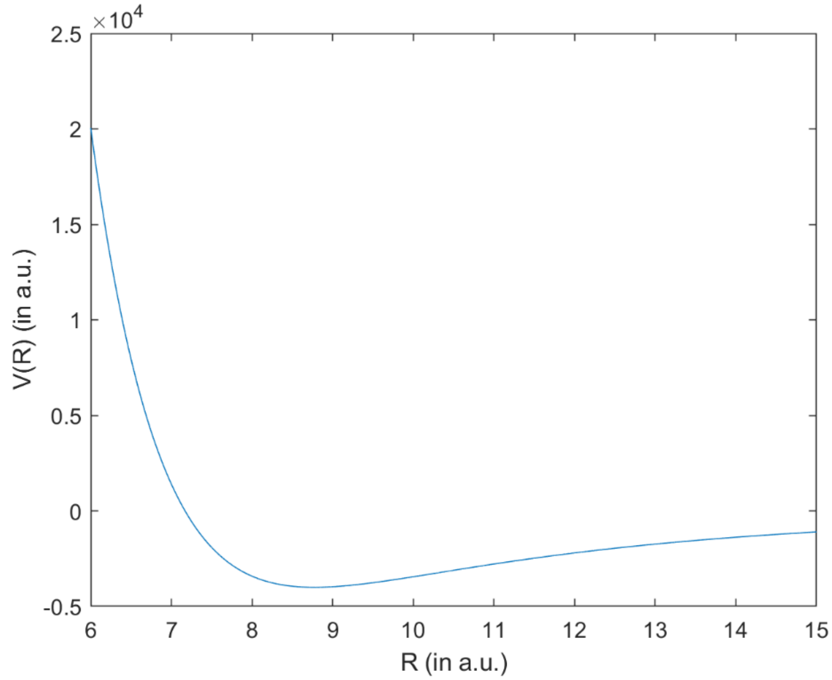

FIG. 2. Potential in (40) as a function of R in a smaller interval

$V(R)$ is a spherically symmetric potential that vanishes as $R \to \infty$, so it matches the case previously discussed, and the Chebyshev numerical method is valid in finding the scattering phase shifts at different energies and partial waves.

IV. Results

Using the MATLAB code with the Chebyshev method, phase shifts were found for different partial waves and ultracold energies. In plots of the phase shifts with respect to different partial wave values, some resonances can be seen, but others are not seen if the code does not detect a problem in the continuity of the curve, as previously discussed. In FIG. 3, one resonance can be seen for the phase shift curve for the energy 10^{-6} a.u. An anomaly can be seen afterwards, which is a resonance that was missed by the code's continuity correction. By reducing the step size between the phase shifts, the resonance can be detected by changing the values of the phase shifts to the "correct" values but keeping them at the same value modulo π. The other resonance can be seen

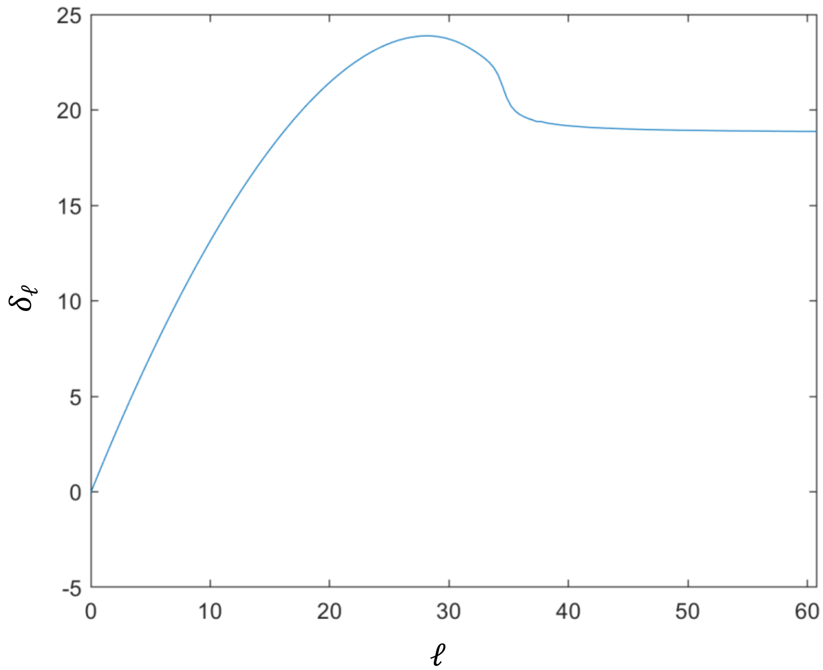

FIG. 3. Phase shifts for the potential in (40) for $E = 10^{-6}$ a.u.

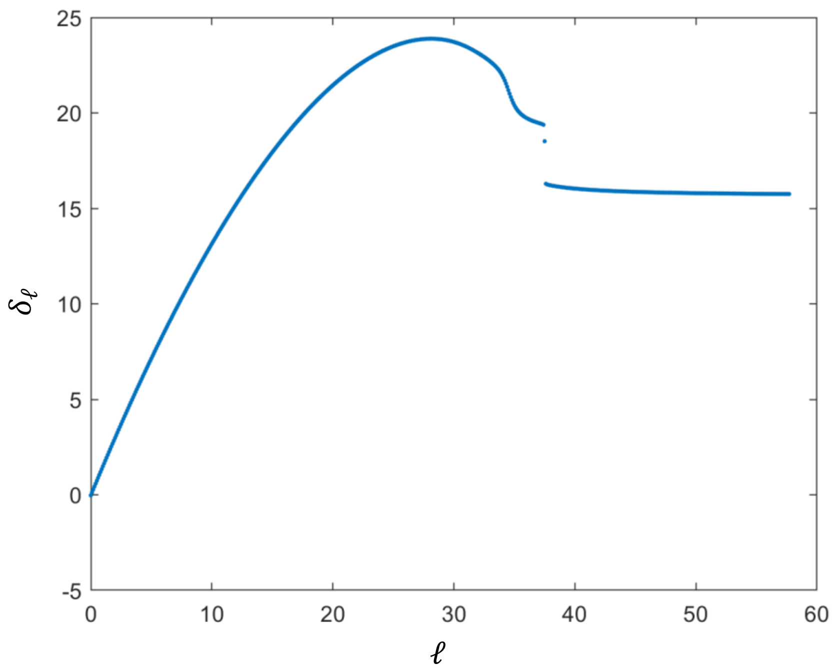

FIG. 4. Phase shifts for the potential in (40) for $E = 10^{-6}$ a.u. with an extra resonance shown

in FIG. 4. The phase shift curves can be plotted for different ultracold energies to show the changes in the shape of the curve and the number of resonances. In FIG. 5, it can be seen that the curves obtain resonances after reaching their maxima, and as energy is increased, these resonances become smaller and broaden out, becoming an imperceptible part of the curve. In order to calculate

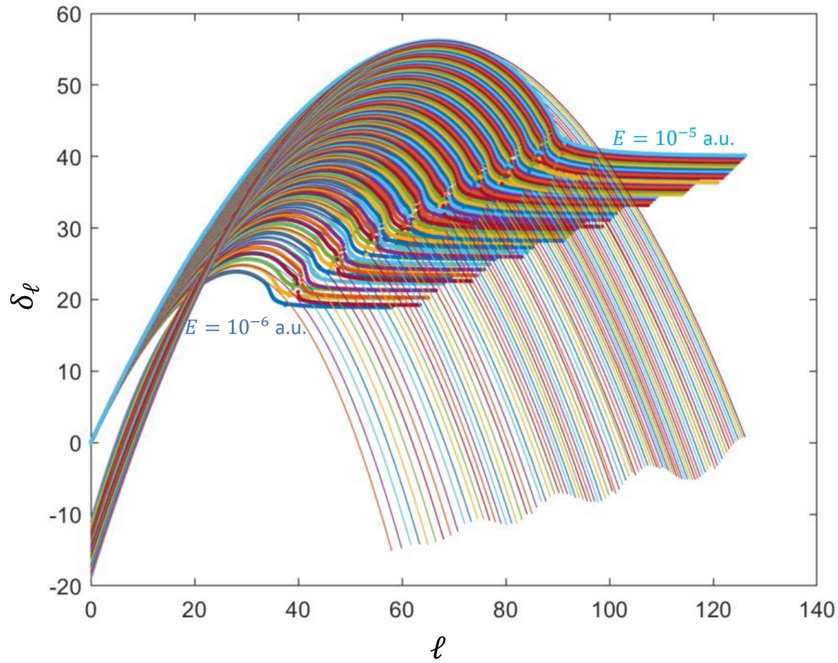

FIG. 5. Phase shifts for the potential in (40) for 91 energy values from 10^{-6} a.u. to 10^{-5} a.u. with an interval $\Delta E = 10^{-7}$, along with 2nd-degree polynomial approximations for the 5 maximum points of the phase shift curves

the broadness and shape of the phase shift curves, 2nd-degree polynomials are approximated for the 5 maximum points of each curve. The 2nd-degree term a for each polynomial shows the broadness of each corresponding phase shift curve. The broadness of the curve seems to oscillate, as seen by the pattern of the polynomial approximations in FIG. 5. This pattern can be seen clearly in FIG. 6 as well. In order to see if the shape of the curve corresponds to the disappearance of resonances, phase shift curves corresponding to energy intervals representing one period of the "oscillation" of a were plotted, as shown in FIG. 7 and FIG. 8, and it was found that each period corresponds to one resonance in the phase shift curve broadening out, becoming imperceptible, and another broadening out to become visible and detected by the continuity correction of the code. Thus the shape of the phase shift curve corresponds directly to the disappearance of resonances.

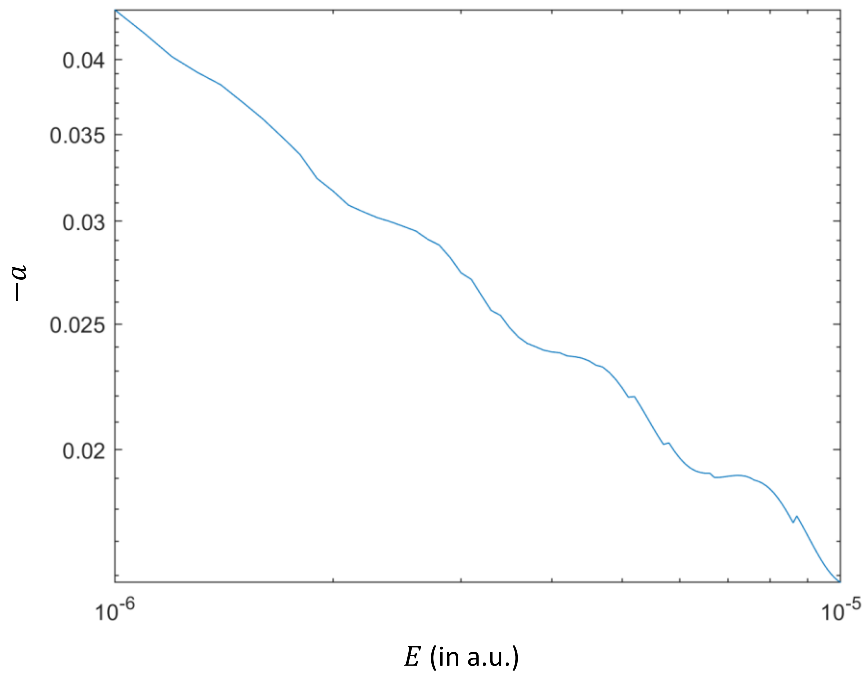

FIG. 6. Positive values of the 2nd-degree coefficient a of the approximated polynomials for the phase shift curves from $E = 10^{-6}$ a.u. to $E = 10^{-5}$ a.u.

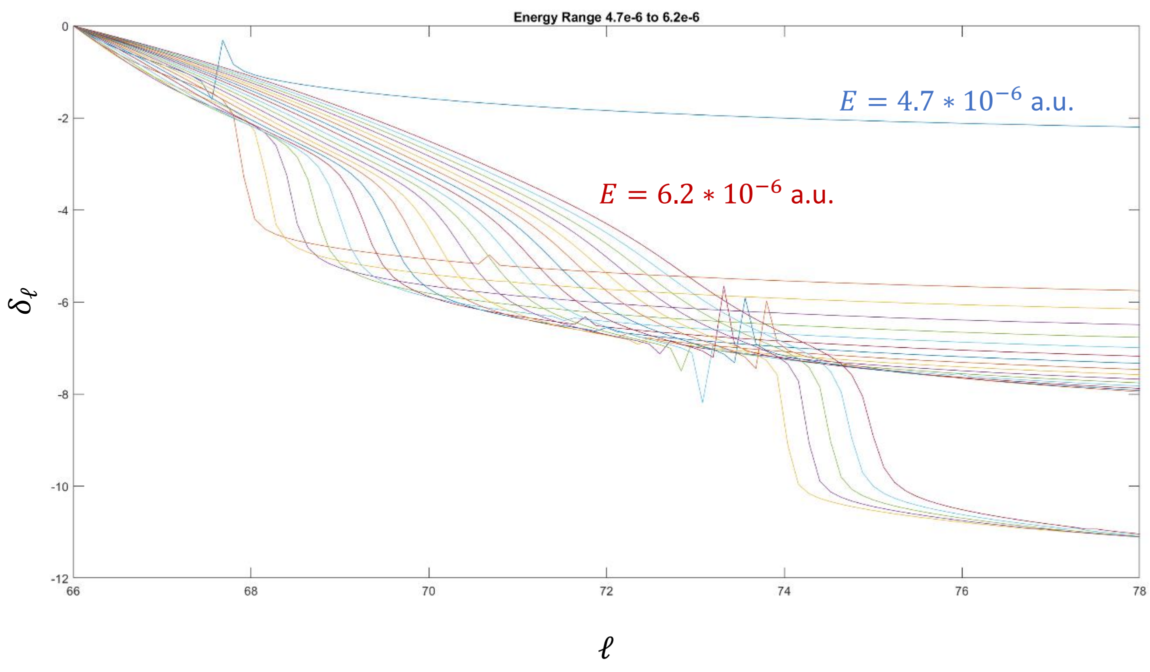

FIG. 7. Phase shifts for the potential in (40) for energy values from $E = 4.7 * 10^{-6}$ a.u. to $E = 6.2 * 10^{-6}$ a.u. with an interval $\Delta E = 7.5 * 10^{-8}$, the energy range for one period of the oscillation of a

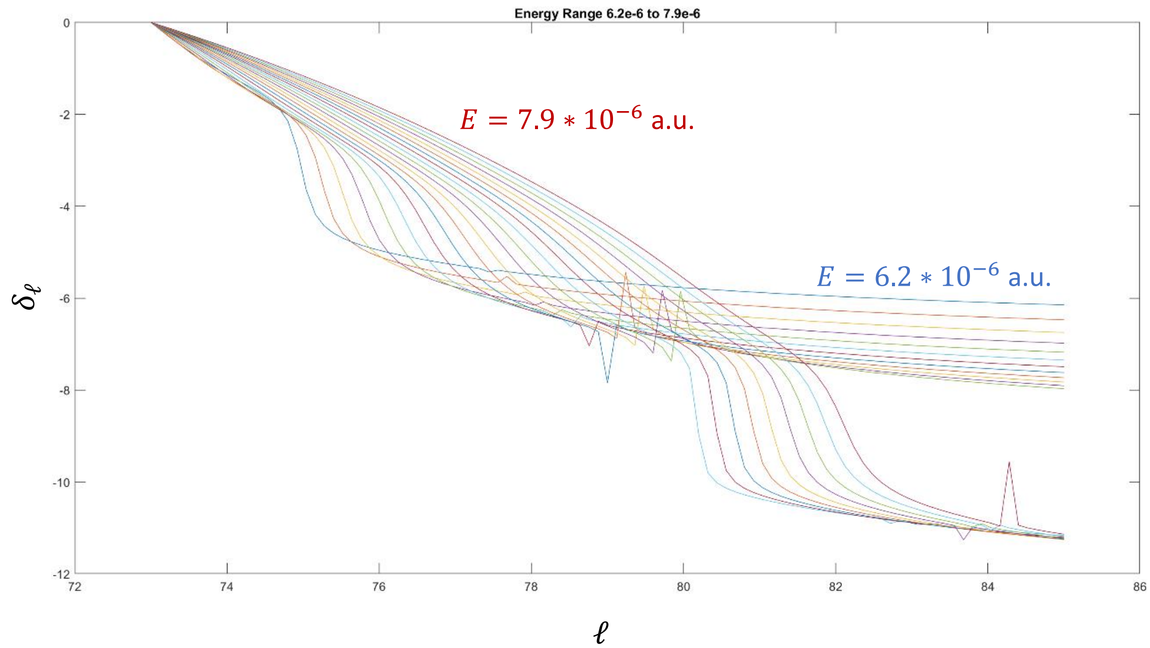

FIG. 8. Phase shifts for the potential in (40) for energy values from $E = 6.2 * 10^{-6}$ a.u. to $E = 7.9 * 10^{-6}$ a.u. with an interval $\Delta E = 8.5 * 10^{-8}$, the energy range for one period of the oscillation of a

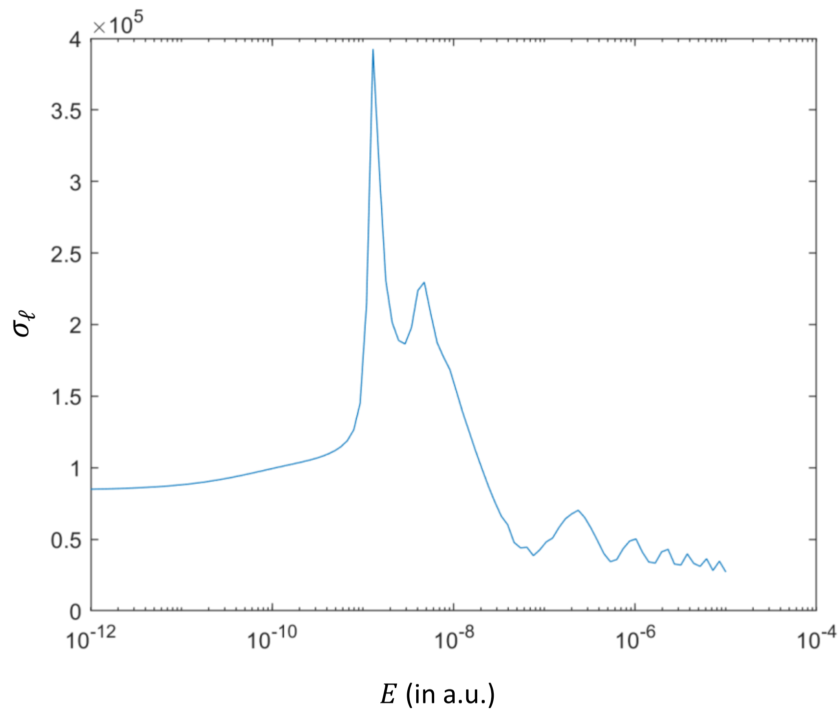

FIG. 9. Cross sections for the potential (40) for energy values from $E = 10^{-12}$ a.u. to $E = 10^{-5}$ a.u.

The scattering cross section σ_ℓ was approximated for a large range of ultracold energies using (24). The terms in the sum approach zero since the values of δ_ℓ approach 0 modulo π for large ℓ. The cross section was approximated by summing the terms up to $\ell = 2.5 * \ell_{max}$, where ℓ_{max} is the value of ℓ where δ_ℓ attains its maximum. As shown in FIG. 9, σ_ℓ attains its maximum at approximately the energy of $1.3 * 10^{-9}$ a.u.

V. Conclusions

The Chebyshev numerical method has been shown to reliably approximate scattering phase shifts and cross sections at ultracold energies. By quantifying the broadness of each phase shift curve with the 2nd-degree term of a 2nd-degree polynomial approximation of the curve, it can be seen that this measurement of broadness oscillates as it corresponds to the disappearance of resonances. Each period of the oscillation corresponds to the reduction and disappearance of one resonance in the phase shift curve. Further investigation could find how the values of the scattering energy correspond to the oscillation, as there appears to be a non-linear correlation.

References

Cote, R., & Dalgarno, A. (1994). Elastic scattering of two Na atoms. Phys. Rev. A, 50, 4827–4835.

Cote, R., & Dalgarno, A. (2000). Ultracold atom-ion collisions. Phys. Rev. A, 62, 012709.

Griffiths, D. J. (2005). Introduction to quantum mechanics. Upper Saddle River, NJ: Pearson Prentice Hall.

Mihaila, B., & Mihaila, I. (2002). Numerical approximations using Chebyshev polynomial expansions: El-gendi's method revisited. Journal of Physics. A, Mathematical and General. 35.

Shu, D. & Simbotin, I. & Côté, R.. (2017). Integral representation for scattering phase shifts via the phase-amplitude approach. Physical Review A. 97. 10.1103/PhysRevA.97.022701.